

Oxidation of H on Rh(111): H₂O product velocity and angular distributions

K. D. Gibson, J. I. Colonell, and S. J. Sibener

The James Franck Institute and the Department of Chemistry, The University of Chicago, Chicago, Illinois 60637

(Received 8 June 1995; accepted 12 July 1995)

The translational energy distribution for the H₂O product from the reaction of H₂ and O₂ on Rh(111) was measured as a function of surface temperature at two different oxygen coverages. The results are well represented by Maxwell–Boltzmann velocity distributions significantly cooler than the surface temperature. For [O]=0.2 monolayers (ML), the product H₂O is slightly faster than for [O]=0.1 ML. The energy distributions are very close to those observed for the trapped and desorbed molecules when scattering low energy H₂O molecular beams from the Rh(111). We also measured the angular dependence of the energy and intensity of the product H₂O at $T_s=650$ K. The velocity distribution of the H₂O product is independent of final angle, and the relative intensities are cosine distributed. © 1995 American Institute of Physics.

INTRODUCTION

The angular and velocity distributions of the products of surface reactions can give incisive information about the dynamics of the reaction path, with particular sensitivity to the last step of the reaction. Many reactions studied so far exhibit an angular variation of product intensity that is peaked as $\cos^n(\Theta)$, with $n \gg 1$.^{1–7} For these systems, it appears that the velocity distribution of the desorbing product flux is also much faster than would be expected for equilibration to the surface temperature.^{1–5,7–9} An exception is the oxidation of deuterium on Pt(111); the angular intensity distribution is cosine, but the final energy is much less than that expected for equilibration to the surface temperature.¹⁰ Recently, similar results were seen for hydrogen and deuterium oxidation on Pd(111).¹¹ A cosine angular intensity distribution is often interpreted as indicating equilibration of the desorbing molecules with the surface, leading to the expectation that the velocity distribution is Maxwell–Boltzmann at the surface temperature. We already knew that for Rh(111) the angular distribution of the H₂O product flux is cosine;¹² with new instrumentation we have now determined the velocity distributions to see how the results compare with this simple prediction, and with the same reaction on Pt(111) and Pd(111).

In our lab, there has been considerable work on the kinetics of hydrogen oxidation on Rh(111).¹² Using multiple molecular beams, it was possible to linearize the reaction, and to determine that a two-step serial process could describe the data. However, it was not possible to definitely ascribe the measured energetics with a particular step in the reaction mechanism. One of the steps has an activation energy of ~ 10 kcal/mol. This is what might be expected for the heat of desorption of water.^{13–15} The energy distribution of the water may give us information as to whether this step is rate limiting; if the water has an energy distribution which indicates that the molecules have not equilibrated to the surface temperature, they probably have spent too short a time on the surface to contribute to the measured kinetics.

EXPERIMENT

These experiments were performed in a scattering machine more thoroughly described elsewhere.^{1,12} The ultrahigh

vacuum (UHV) scattering chamber contains the crystal manipulator and an independently rotatable and differentially pumped quadrupole mass spectrometer with an angular resolution of 1°. Critical to these experiments was the ability to measure the velocities of the product H₂O separately from any surface residence time. To accomplish this, we attached to the rotatable mass spectrometer a cross-correlation chopper which intercepts the product flux between the crystal and the detector. This consists of a housing which contains an ac hysteresis motor evacuated by an 11 //s ion pump. The shaft of the motor extends through a differential pumping region, also evacuated by an 11 //s ion pump, and then into the UHV chamber, where the chopper is keyed to it. This chopper interrupts the flux of molecules leaving the crystal surface at a distance of 10.5 cm from the electron-impact ionizer of the mass spectrometer. A slotted disk attached to the shaft interrupts the light between a small incandescent bulb and a photodiode, providing the timing signal to trigger the counting electronics.

The cross-correlation chopper was made using a 511 channel pattern derived in our group.¹⁶ During the time-of-flight (TOF) experiments described in this paper, the chopper speed was 195.69 Hz, corresponding to channel times of 10 μ s. The signal was acquired by a pair of Ortec ACE-MCS (multichannel scalar) boards, counting on alternate chopper cycles, controlled by custom CAMAC hardware. Two scalars were used because they did not immediately reset at the end of each pass. Counting times were typically 8.5 min (10⁵ cycles), though sometimes we counted for up to 24 min to improve our statistics for the weaker signals.

Analysis was done by first deconvoluting the measured spectrum with a function that was the convolution of the rectangular chopper slots and the round detector apertures. This function was determined by shining a light through the detector when the machine was vented and the chopper was running. The result was further analyzed utilizing a nonlinear least-squares fitting routine, which convoluted a Maxwell–Boltzmann velocity distribution with the instrumental broadening function attributable to the finite length of the ionizer.

The rhodium crystal was cut and polished to within a degree of the (111) plane, as confirmed with Laue x-ray

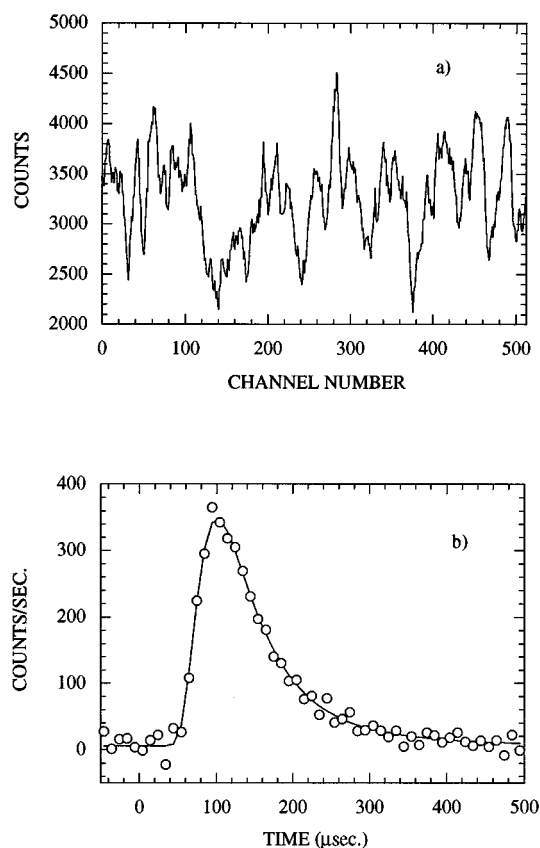


FIG. 1. A TOF spectrum for the production of H_2O : $\Theta_i=45^\circ$, $\Theta_f=0^\circ$, $T_s=650$ K, and $[\text{O}]=0.1$ ML. Panel (a) shows the data from the 511 channel cross-correlation chopper, and panel (b) shows the same data after deconvolution with the cross-correlation pattern. The solid line in panel (b) is the convolution of a Maxwell–Boltzmann velocity distribution ($T_g=586$ K) and the instrumental broadening.

backreflection. Initially, the crystal was cleaned by Ar^+ ion bombardment ($10 \mu\text{A}$, 900 K), followed by annealing at 1300 K. This served to remove contaminants such as sulfur and boron. Carbon was another common contaminant, at least partially due to background adsorption, but could easily be removed by exposing the crystal to oxygen with the surface at 900 K. Cleanliness was confirmed with Auger spectroscopy and surface flatness by the specular reflection of a He beam. Since Rh at elevated temperatures adsorbs oxygen, the crystal was heated to 1300 K for 3 min between spectra to remove all of the oxygen.

Continuous beams of hydrogen and oxygen were made by separate supersonic expansions in the source chamber. This chamber is divided internally into two parts, so that separate pumps were used for the two gases. The beams are in a plane perpendicular to the scattering plane defined by the rotating detector, with one in the scattering plane, and the other inclined by 15° , with the resultant beam spots overlapping at the position of the crystal. The crystal can be moved out of the path of the center beam, and the detector rotated so that the energy distribution of the center beam can be measured directly.

These experiments were done at a known oxygen coverage, established by adjusting the relative flux of the two

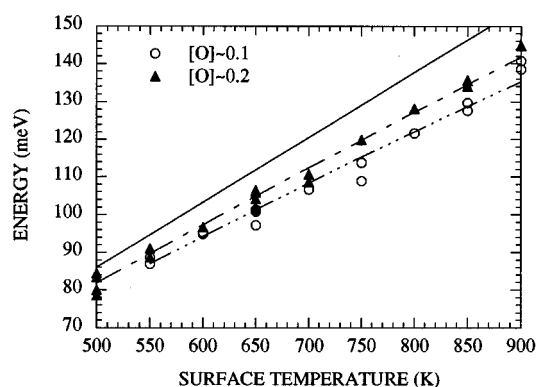


FIG. 2. The average energies of the Maxwell–Boltzmann velocity distributions used to fit data taken as a function of T_s with $\Theta_i=45^\circ$, $\Theta_f=0^\circ$; circles are for data taken with $[\text{O}]=0.1$ ML and the triangles are for data taken with $[\text{O}]=0.2$ ML. The broken lines through the points are from fits to the data with $T_w=(6.15\pm 0.5)\times 10^3$ K for $[\text{O}]=0.1$ ML and $T_w=(9.5\pm 0.9)\times 10^3$ K for $[\text{O}]=0.2$ ML (see the text). The solid line is the expected energy if $T_g=T_s$.

beams at each surface temperature. This coverage was checked by titration. First, we established a steady-state coverage with both beams on, and then flagged off the oxygen beam while monitoring the H_2O signal. The integrated signal was compared with that of a saturation layer of oxygen, 0.5 monolayers (ML).¹⁷ We looked at two oxygen coverages, ~ 0.1 (0.09 ± 0.03) and ~ 0.2 (0.22 ± 0.04) ML. 0.3 ML was tried, but the product signal was very weak. At the temperatures and coverages of these experiments, the oxygen is disordered.^{18–20}

We do not know the hydrogen coverage; it is not 0, since H_2O production is a Langmuir–Hinshelwood reaction.¹² However, hydrogen desorbs rapidly at the temperatures of these experiments,^{21,22} too rapidly for us to measure the coverage by the titration procedure, and adsorbed oxygen interferes with hydrogen adsorption.²³ Therefore, we feel confident that the hydrogen coverage is low for all of our experiments, certainly lower than the oxygen coverage.

RESULTS

Figure 1 shows a TOF spectrum taken with the detector at $\Theta_f=0^\circ$ relative to the surface normal, both before and after deconvolution for the cross-correlation pattern. The solid line in panel (b) is a nonlinear least-squares fit to a Maxwell–Boltzmann velocity distribution:

$$f(v) \propto v^3 \exp\left(-\frac{m_g v^2}{2k_B T_g}\right), \quad (1)$$

convoluted with the instrumental broadening function. Here, m_g is the mass of H_2O , k_B is Boltzmann's constant, and T_g is the temperature of the gas. For this experiment, $T_g=586$ K, while the surface temperature, T_s , was 650 K.

Figure 2 shows the average energies of the measured Maxwell–Boltzmann velocity distributions at $\Theta_f=0^\circ$, as a function of T_s for two different oxygen coverages ($[\text{O}]=0.1$ and 0.2 ML). Also shown is the expected energy of the product H_2O , $2k_B T_s$, if it were equilibrated to T_s . The H_2O trans-

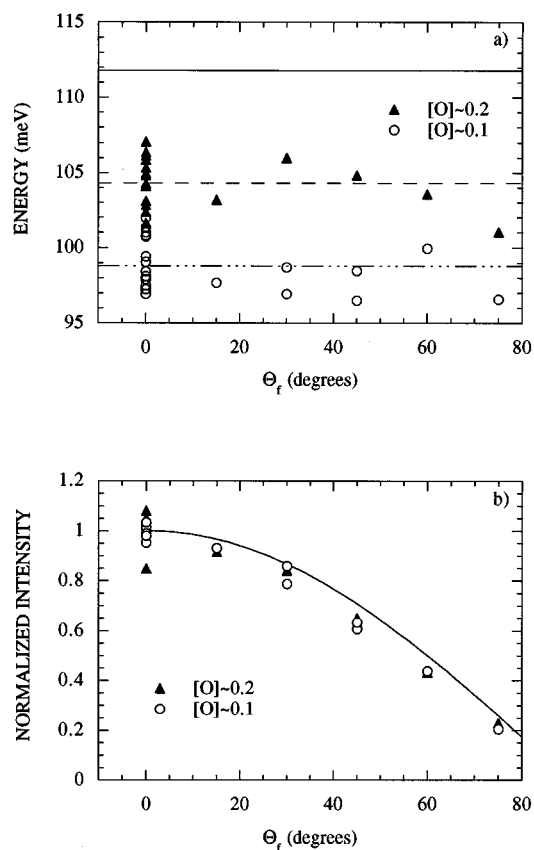


FIG. 3. The angular dependence of the average energies and relative intensities of the Maxwell-Boltzmann velocity distributions used to fit data taken at $T_s=650$ K and $\Theta_i=45^\circ$. Panel (a) shows the energies for $[O]=0.1$ ML (circles, average energy of 98.8 ± 0.8 meV) and $[O]=0.2$ ML (triangles, average energy of 104.3 ± 0.9 meV). The solid line is the energy expected if $T_g=T_s$, 112 meV. Panel (b) shows the intensities of the velocity distributions normalized to the average of the data taken at $\Theta_f=0^\circ$. The solid line is what is expected for a cosine angular distribution.

lational energy for $[O]=0.2$ ML was slightly higher than for $[O]=0.1$ ML; but in both cases, T_g was less than T_s . Also, the deviation between T_g and T_s increases slightly with surface temperature.

The differences between the experimental Maxwell-Boltzmann velocity distributions plotted in Fig. 2 and what would be expected for equilibration to the surface temperature is not large. We carefully checked our fitting procedure and TOF calibration by using effusive beams of O_2 and He, generated using pressures of $1-2 \times 10^{-6}$ Torr behind an 0.080 in. aperture. For these calibration runs, the detector was rotated to directly view the effusive beam. The results confirm that our above stated results are valid: the desorbing H_2O is significantly cooler than T_s .

We investigated the angular variation of the energy and intensity of the H_2O product molecules at $T_s=650$ K. The results are shown in Fig. 3. Panel (a) shows the product translational energy as a function of final scattering angle, Θ_f . Again, it appears that the higher oxygen coverage results in a higher product translational energy while both coverages exhibit an energy that is less than $2k_B T_s$. The angular variation of the H_2O product intensity is shown in panel (b), along

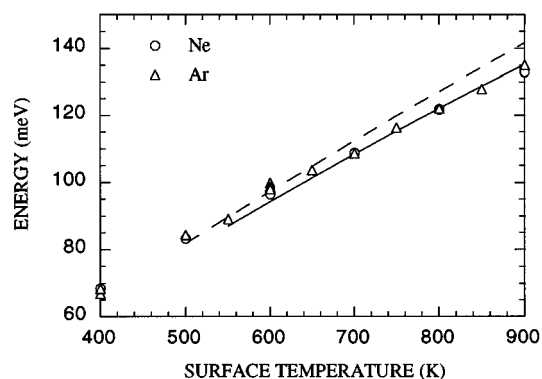


FIG. 4. The average energy of the Maxwell-Boltzmann velocity distributions used to fit scattered H_2O , with $\Theta_i=55^\circ$ and $\Theta_f=-10^\circ$. The different symbols are for the two different seed gases: Ne (average energy of the incident H_2O , $\langle E \rangle$, equal to 63.1 meV) and Ar ($\langle E \rangle=34.9$ meV). The two lines are the fits shown in Fig. 2 for the reactively produced H_2O .

with a line showing the expected value if the relative intensities vary as $\cos(\Theta_f)$. The intensities may be slightly more peaked than cosine, but a cosine fit is within our error.

We also looked at the trapping of water on Rh(111); the results are shown in Fig. 4. These experiments were done with an incident angle, Θ_i , of 55° , and $\Theta_f=-10^\circ$ (65° from the specular scattering angle). The H_2O beams used were made by bubbling an inert gas through a reservoir of water. We used Ne (the average energy of the incident water, $\langle E \rangle$, equal to 63.1 meV) and Ar ($\langle E \rangle=34.9$ meV). Near specular (within 1°), we found a significant signal due to trapped and desorbed H_2O , as well as a direct inelastic signal. Using Ar as the seed gas, and with $T_s=600$ K, the integrated intensity of the H_2O trapped and desorbed channel was ~ 3 times that of the direct inelastic channel. Far from specular, where the signal we detected was dominated by trapped and desorbed molecules, the results were easily fit with a single Maxwell-Boltzmann velocity distribution. It appears that the trapped and desorbed molecules in the seeded beam experiments had energies close to those of the H_2O product molecules. There may be a deviation towards lower energies at the higher temperatures, but the results may be biased by a small amount of direct inelastic scattering. Also, there is no oxygen and hydrogen on the surface during these scattering experiments.

DISCUSSION

For many surface reactions, the translational energy of the product molecules is much greater than $2k_B T_s$. This behavior is characteristic of reactive potential energy surfaces with exit channel barriers and, perhaps, low adsorption energies for the reaction products. However, for hydrogen oxidation on either Pt(111), Pd(111), or Rh(111), the H_2O product translational energy is cooler than $2k_B T_s$. Water is formed by a Langmuir-Hinshelwood mechanism, but we do not know the precise steps leading to H_2O formation at our coverages; is it $H+OH$, the disproportionation of OH , or both? In either case, there is at least 10–20 kcal/mol (430–860 meV per molecule) available after the reaction;²⁴ we measure only a fraction of this energy in translation. In fact, the en-

ergy is very close to that of the trapped and desorbed molecules from the scattering experiments. This suggests that none of the energy released by the reaction shows up in the translational energy of the product molecules. The angular distribution of the intensity of the H₂O product molecules, being nearly cosine, is also different than for many other reactions, where the intensities are more highly peaked in the normal direction.

Our results are consistent with experiments that measured the velocity and angular distributions of desorbing molecules involving systems with nonactivated adsorption.^{25,26} That the energy is less than $2k_B T_s$ is actually a dynamical effect due to the inefficient energy exchange with the surface.²⁷ If this is true, then, by detailed balance, the higher the incident energy of an incoming molecule, the less likely it is to stick. We find this to be qualitatively true for the seeded H₂O beams we used during the trapping experiments. Near specular, there was a clearly resolved trapping and desorption component, along with direct but inelastically scattered water, when seeding with Ar ($\langle E \rangle = 34.9$ meV) or Ne ($\langle E \rangle = 63.1$ meV). When He was used ($\langle E \rangle \approx 230$ meV), there was no clearly resolved signal due to trapping and desorption. That the product molecules appear to be trapped on the surface provides some indication that they spend enough time on the surface to contribute to the measured reaction kinetics, and therefore might account for the 10 kcal/mol step already mentioned.

That the velocity distributions indicate trapping and desorption of the product H₂O molecules suggests using a simple model for parametrizing the data shown in Fig. 2. This consists of a Maxwell–Boltzmann velocity distribution at the surface temperature, multiplied by a trapping probability that falls off exponentially with velocity.²⁸

$$f(v) \propto v^3 \left[\exp\left(-\frac{m_g v^2}{2k_B T_g}\right) \right] \left[\exp\left(-\frac{m_g v^2}{2k_B T_w}\right) \right], \quad (2)$$

where

$$\frac{1}{T_w} = \frac{1}{T_g} - \frac{1}{T_s}. \quad (3)$$

The broken lines in Fig. 2 are the results of fitting the data to Eq. (3), giving values for T_w of $(6.15 \pm 0.5) \times 10^3$ K for $[O] = 0.1$ ML, and $(9.5 \pm 0.9) \times 10^3$ K for $[O] = 0.2$ ML. Figure 5 shows the comparison of two Maxwell–Boltzmann velocity distributions, one with $T_g = 650$ K and the other with $T_g = 588$ K. The first distribution is what would be predicted for a surface temperature of 650 K, if the H₂O came off at the surface temperature. The second distribution is what would be predicted by Eq. (2) for $T_s = 650$ K and $[O] = 0.1$ ML. Also shown are the relative values of the velocity-dependent trapping probability, the second exponential term in Eq. (2). That the angular intensity variation is cosine and the velocity distribution is independent of angle shows that the desorbing molecules have both components of velocity (parallel and perpendicular to the surface) equilibrated.²⁹ For the case of the reactively produced H₂O, the equilibration of the parallel component of velocity is probably helped by the presence of the disordered oxygen atoms, making the Rh(111) surface rougher. It is also possible that the higher

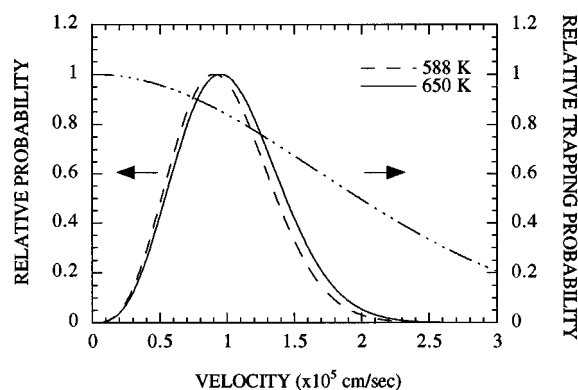


FIG. 5. A comparison of two Maxwell–Boltzmann velocity distributions. The distribution with $T_g = 650$ K (solid line) is what would be predicted for a surface temperature of 650 K, if the H₂O came off at the surface temperature. The distribution with $T_g = 588$ K (dashed line) is what would be predicted by Eq. (2) for $T_s = 650$ K and $[O] = 0.1$ ML. The dot-dash line shows the relative values of the velocity-dependent trapping probability, the second exponential term in Eq. (2).

value of T_w for the higher oxygen coverage reflects an increased softness of the surface; for low velocity molecules, the major way that energy is exchanged with the surface is through phonons.

The results for Rh(111) differ somewhat from those of hydrogen and deuterium oxidation on Pt(111)¹⁰ and Pd(111).¹¹ For Pt(111), it was observed that the mean D₂O translational energy was not only much less than expected for equilibration of the product D₂O to the surface temperature [$\langle E \rangle = 49$ meV ($\langle E \rangle / 2k_B = 283$ K) at $T_s = 664$ K], but was nearly independent of T_s . For Pd(111), the translational energy of product H₂O was independent of surface temperature for T_s between 430 and 710 K, with $\langle E \rangle = 49$ meV ($\langle E \rangle / 2k_B = 284$ K). For this surface, there were also measurements on the internal states of the product D₂O. The energy in rotation corresponded very closely to the surface temperature. It was also concluded that only a small number of the product D₂O molecules were vibrationally excited. Foner and Hudson³⁰ concluded that the product H₂O from the oxidation of hydrogen on polycrystalline Pt had no excess vibrational energy at $T_s = 1273$ K. All of these systems exhibit the same basic result that we observe for Rh(111): much of the excess energy of this exoergic reaction is not carried away from the surface by the product water molecules.

SUMMARY

We have investigated the formation of water on a Rh(111) single crystal at two different oxygen coverages ($[O] = 0.1$ and 0.2 ML), and for surface temperatures between 500 and 900 K. Constant oxygen coverage was carefully maintained by varying the relative intensities of the continuous H₂ and O₂ beams. This allowed us to adjust our coverage of any surface temperature, even though the kinetics of the reaction varied with the temperature. For both coverages, the translational velocities of the H₂O product at $\Theta_f = 0^\circ$ are well represented by Maxwell–Boltzmann distributions signifi-

cantly cooler than $2k_B T_s$. There is a small effect due to oxygen coverage; the translational energies are slightly higher at the larger coverage. We also measured the angular dependencies of the product H₂O velocity distributions and intensity at $T_s=650$ K. The velocity distributions are independent of angle, while the intensity has a cosine angular dependence. We also looked at the scattering of rare gas seeded beams of H₂O. The velocity distributions of the trapped and desorbed H₂O are very close to those of the reactively produced H₂O; they are fit by Maxwell-Boltzmann distributions which are also cooler than $2k_B T_s$. We conclude that the excess energy of the H₂+O₂/Rh(111) reaction is not carried away from the surface as translational energy of the product H₂O. Instead, it appears that once formed, the H₂O is transiently trapped on the surface. That the translational energy of the desorbing molecules is less than $2k_B T_s$ is reasonable for a physisorbed system with no barrier to adsorption. Using detailed balance, we expect that molecules with lower translational velocities have a greater probability of exchanging enough energy with the surface phonons to become trapped. The trapping also scales with total energy, implying that the H₂O spends enough time on the surface for both the perpendicular and parallel components of velocity to equilibrate.

ACKNOWLEDGMENTS

Acknowledgment is made to the donors of The Petroleum Research Fund, administered by the ACS, for partial support of this research. This work was also supported in part by the Materials Research Science and Engineering Center Program of the National Science Foundation under Award No. DMR-9400379. J.I.C. also thanks AT&T Bell Laboratories for financial support through the Graduate Research Program for Women.

- ¹J. I. Colonell, K. D. Gibson, and S. J. Sibener, *J. Chem. Phys.* (in press).
- ²L. S. Brown and S. J. Sibener, *J. Chem. Phys.* **90**, 2807 (1989).
- ³E. Poehlmann, M. Schmitt, H. Hoinkes, and H. Wilsch, *Surf. Sci.* **287**, 269 (1993).
- ⁴G. Comsa, R. David, and B.-J. Schumacher, *Surf. Sci.* **85**, 45 (1979).
- ⁵L. K. Verheij, M. B. Hugenschmidt, A. B. Anton, B. Poelsma, and G. Comsa, *Surf. Sci.* **210**, 1 (1989).
- ⁶C. T. Rettner, H. A. Michelsen, D. J. Auerbach, and C. B. Mullins, *J. Chem. Phys.* **94**, 7499 (1991).
- ⁷Y. Ohno, T. Matsushima, and H. Uetsuka, *J. Chem. Phys.* **101**, 5319 (1994).
- ⁸G. Comsa, R. David, and B.-J. Schumacher, *Surf. Sci.* **95**, L210 (1980).
- ⁹C. A. Becker, J. P. Cowin, L. Wharton, and D. J. Auerbach, *J. Chem. Phys.* **67**, 3394 (1977).
- ¹⁰S. T. Ceyer, W. L. Guthrie, T.-H. Lin, and G. A. Somorjai, *J. Chem. Phys.* **78**, 6982 (1983).
- ¹¹A. de Meijere, K. W. Kolosinski, and E. Hasselbrink, *Faraday Discuss.* **96**, 265 (1993).
- ¹²D. F. Padowitz and S. J. Sibener, *Surf. Sci.* **254**, 125 (1991).
- ¹³J. J. Zinck and W. H. Weinberg, *J. Vac. Sci. Technol.* **17**, 188 (1980).
- ¹⁴P. A. Thiel and T. E. Madey, *Surf. Sci. Rep.* **7**, 211 (1987).
- ¹⁵J. Kiss and F. Solymosi, *Surf. Sci.* **177**, 191 (1986).
- ¹⁶D. D. Koleske and S. J. Sibener, *Rev. Sci. Instrum.* **63**, 1 (1992).
- ¹⁷C. T. Reimann, M. El-Maazawi, K. Walzl, B. J. Garrison, N. Winograd, and D. M. Deaven, *J. Chem. Phys.* **90**, 2027 (1989).
- ¹⁸P. A. Thiel, J. T. Yates, and W. H. Weinberg, *Surf. Sci.* **82**, 22 (1979).
- ¹⁹J. T. Yates, P. A. Thiel, and W. H. Weinberg, *Surf. Sci.* **82**, 45 (1979).
- ²⁰K. A. Peterlinz and S. J. Sibener (submitted).
- ²¹J. T. Yates, P. A. Thiel, and W. H. Weinberg, *Surf. Sci.* **84**, 427 (1979).
- ²²D. F. Padowitz and S. J. Sibener, *J. Vac. Sci. Technol. A* **9**, 2289 (1991).
- ²³P. A. Thiel, J. T. Yates, and W. H. Weinberg, *Surf. Sci.* **90**, 121 (1979).
- ²⁴M. A. Van Hove, W. H. Weinberg, and C.-M. Chan, *Low-Energy Electron Diffraction* (Springer-Verlag, Berlin, 1986).
- ²⁵C. T. Rettner, E. K. Schweizer, and C. B. Mullins, *J. Chem. Phys.* **90**, 3800 (1989).
- ²⁶K.-H. Allers, H. Pfnür, P. Feulner, and D. Menzel, *Surf. Sci.* **291**, 167 (1993).
- ²⁷J. C. Tully, *Surf. Sci.* **111**, 461 (1981).
- ²⁸J. E. Hurst, Jr., L. Wharton, K. C. Janda, and D. J. Auerbach, *J. Chem. Phys.* **83**, 1376 (1985).
- ²⁹M. Head-Gordon, J. C. Tully, C. T. Rettner, C. B. Mullins, and D. J. Auerbach, *J. Chem. Phys.* **94**, 1516 (1991).
- ³⁰S. N. Foner and R. L. Hudson, *J. Vac. Sci. Technol. A* **1**, 1261 (1983).